Influence of BTA on Electrochemical Behavior of AgCu50 Alloy

Vesna Grekulović[1], Mirjana Rajčić-Vujasinović[1,*], Batrić Pešić[2], Zoran Stević[1]

[1] University of Belgrade, Technical Faculty in Bor, V.J. 12, 19210 Bor, Serbia
[2] University of Idaho, USA
*E-mail: mrajcic@tf.bor.ac.rs

Electrochemical behavior of AgCu50 alloy (50 mass.% Ag + 50 mass.% Cu) was investigated by cyclic voltammetry and potentiostatic methods in 0.1 mol/dm^3 NaOH solution containing BTA in different concentrations (0.00005 – 0.01 mol dm^{-3}). Potentiostatic oxidation was followed by SEM and EDS analysis of electrode surface. The presence of benzotriazole influenced the potential and the hight of current peaks. Increasing of BTA concentration leads to the decreasing of current in investigated potential range. Heights of current peaks point at electrode surface coverage with adsorbed BTA molecules. Based on the assumption that the adsorption was governed by Langmuir isotherm and using the dependence $C/\theta = f(C_{BTA})$, the calculated Gibbs energy of adsorption of BTA on investigated AgCu50 alloy was -27 kJ mol^{-1}.

1. INTRODUCTION

Organic inhibitors are extensively used in protection of metals and alloys from corrosion in different environments. The azoles, due to their high efficiency for protection of copper based materials [1], have been widely investigated, among which benzotriazole (1-H-benzotriazole, $C_6H_4N_3H$) has been proven as the most accepted. For convenience, this neutral molecule has been commonly denoted by BTAH or BTA acronym, where 1-H signifies H atom attached to the N1 atom in the triazole group. BTA is an anodic copper corrosion inhibitor, whose protective mechanism involves the chemisorption on copper surface, governed by the Langmuir isotherm [2-6], followed by formation of Cu(I)BTA complex [7-15].

Adsorption of BTA on copper surface can be described with the following reactions [16, 17]:

$$Cu + BTA \rightarrow (Cu\text{-}BTA)_{ads} \tag{1}$$

$$BTA_{aq} + xH_2O_{ads} \rightarrow BTA_{ads} + x\ H_2O_{aq} \tag{2}$$

Abdulah et al. [7] suggest that the mechanism of formation of Cu(I)BTA complex on copper surface consists of the following reactions:

$$Cu_{(s)} + BTAH_{(aq)} = Cu:BTAH_{(ads)} \tag{3}$$

where $Cu:BTAH_{(ads)}$ represents BTAH adsorbed on copper surface. Cu:BTAH can be oxidized by anodic polarization to the complex which has protective characteristics, by the following reaction:

$$Cu:BTAH_{(ads)} = Cu(I)BTA_{(s)} + H^+_{(aq)} + e^- \tag{4}$$

Modestov et al. [3] suggest that in parallel with the formation of CuBTA film, beneath, the formation of copper(I) oxide [Cu_2O] and copper(II) oxide [CuO] films is also occurring.

Tromans [15] has constructed an E_h-pH diagram for Cu-BTA systems, which enables to predict the protective influence of BTA as a function of its concentration, pH and redox potential.

The inhibition of silver has rarely been discussed in available literature [18, 19]. Hope et al. [18] investigated the behavior of silver in cyanide solution in the presence of 2-mercaptobenzothiasole and confirmed the formation of AgMBT complex. Rajeswaran et al. [19] has studied the crystalline structure of silver-benzotriazole nanoprecipitates. It was found that each nitrogen atom in triazole participates in bonding to a separate silver atom, creating a polymeric, highly insoluble, AgBTA complex. Based on literature data, it can be assumed that in alkaline solutions, the presence of benzotriazole leads to the formation of AgBTA complex as well as the oxides of silver, silver(I) oxide [Ag_2O] and silver(II) oxide [AgO].

The aim of the present work is to study behavior of AgCu50 alloy in 0.1 mol dm^{-3} NaOH in the presence of benzotriazole by using different electrochemical methods. The electrode microstructure was characterized by scanning electron microscopy (SEM) and energy-dispersive x-ray spectroscopy (EDS) analysis.

2. EXPERIMENTAL

The experiments were carried out in a system consisting of an electrochemical cell and hardware interface for computerized control and data acquisition. In a standard three-electrode electrochemical cell, the working electrode was AgCu50 alloy, whose potential was controlled against saturated calomel reference electrode (SCE). Platinum foil served as a counter electrode. The computerized control (National Instruments card, NI-6251) and data acquisition software (LabVIEW 8.2 platform), fully developed by Technical Faculty in Bor [20], was used to run the electrochemical experiments.

The investigations were performed at 25°C in 0.1M NaOH in the absence and the presence (5x10^{-5} mol dm^{-3} – 1x10^{-2} mol dm^{-3}) of BTA (reagent grade- "Kraemer and Martin GMBH", Duisburg,

Germany), using cyclic voltammetry, open circuit potential measurement and potentiostatic methods. Cyclic voltammograms were recorded in a potential range from -1.6 V to +1 V (SCE) with a scan rate of 20 mV/s. Potentiostatic experiments were performed at anodic peaks potentials. After potentiostatic oxidation, the electrode surface was characterized by SEM (Tescan, Vega II) equipped with SDD (Silicon Drift Detector), which requires no liquid nitrogen for cooling and can accept large amounts of x-rays to create very fast x-ray maps. Digital Imaging, X-ray Elemental Mapping, and X-ray Spectra, are all computer controlled through the IXRF software (Iridium Ultra[TM]) and hardware.

The alloy AgCu50 (50mass.% Ag + 50mass.% Cu), for the working electrode, was obtained by melting aliquots of pure Ag and Cu powder in a quartz furnace at 1250 °C, subsequent casting and cooling in air. Cast alloy was treated with aqueous solution of HNO_3 (1:1) in a goal to remove oxides formed during cooling. Upon rolling, the 1-milimeter diameter wire was obtained by drawing. After annealing at 600°C for 30 min, the wire was cut into 15 cm long pieces, and used individually for working electrode preparation, which included the following steps, bending 1-cm long end at 90° (L-shaped wire), casting in an epoxy resin, and polishing. By polishing on a metallographic paper, the opened L-section of copper wire was rectangular in shape, with the dimension of 1cm long and 0.1cm in diameter, giving 0.1 cm^2 for an active surface area of working electrode.

3. RESULTS AND DISCUSSION

3.1. Cyclic voltammetry

The effect of BTA concentration on cyclic voltammetry of AgCu50 was studied in the concentration range 0-0.01 mol dm^{-3} BTA. To enable a more effective overview, the results are presented in two figures, according to the concentration range of BTA. The lower concentration range, 5.0×10^{-4}- 5.0×10^{-3} mol dm^{-3} BTA, is represented by Figure 1, while the higher concentration range data, 1.0×10^{-3} - 1.0×10^{-2} mol dm^{-3}, are given in Figure 2. Each of these two figures also contain the control cyclic voltammograms, i.e. the conditions without BTA addition. All experiments were performed in 0.1 mol dm^{-3} NaOH, at the scannig rate of 20 mV s^{-1}.

In the control voltammograms, no addition of benzotriazole, the anodic branch has six current waves, all matched by six corresponding cathodic current waves, plus one additional anodic current wave in the cathodic half of the voltammogram. The adsorption of hydroxyl ions is considered as the first reaction step that can take place during the anodic polarization of AgCu50 alloy and it is attributed to current wave A_1 [21-27]. Current peaks A_2 and A_3 correspond to the formation of copper oxides Cu_2O and CuO, respectively [22, 25, 28-32]. Current peaks A_4 and A_5 are assigned to the formation of silver (I) oxide, first of Ag_2O type-I, and then Ag_2O type-II [33-40]. The formation of silver (II) oxide, AgO, is represented by peak A_6. In the cathodic direction, the anodic reaction products are sequentially reduced in the corresponding reverse order, C_6, C_5, C_4, C_3, C_2, and C_1. Anodic current wave A_7, on the cathodic part of voltammograms, is associated with the oxidation of elemental silver to Ag_2O [41].
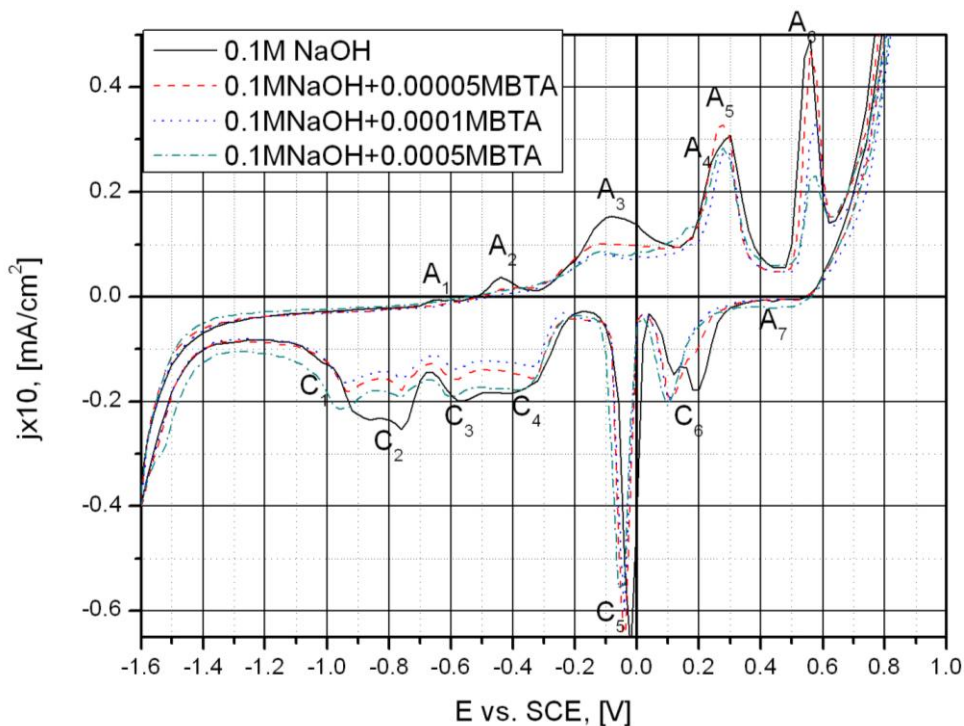
Figure 1. Cyclic voltammetry of AgCu50 in the lower concentration range of BTA, 5.0×10^{-4}- 5.0×10^{-3} mol dm^{-3}. The solid line voltammogram represents the control conditions, the absence of BTA. All voltammograms are produced in 0.1M NaOH at 20 mV s^{-1} scan rate.
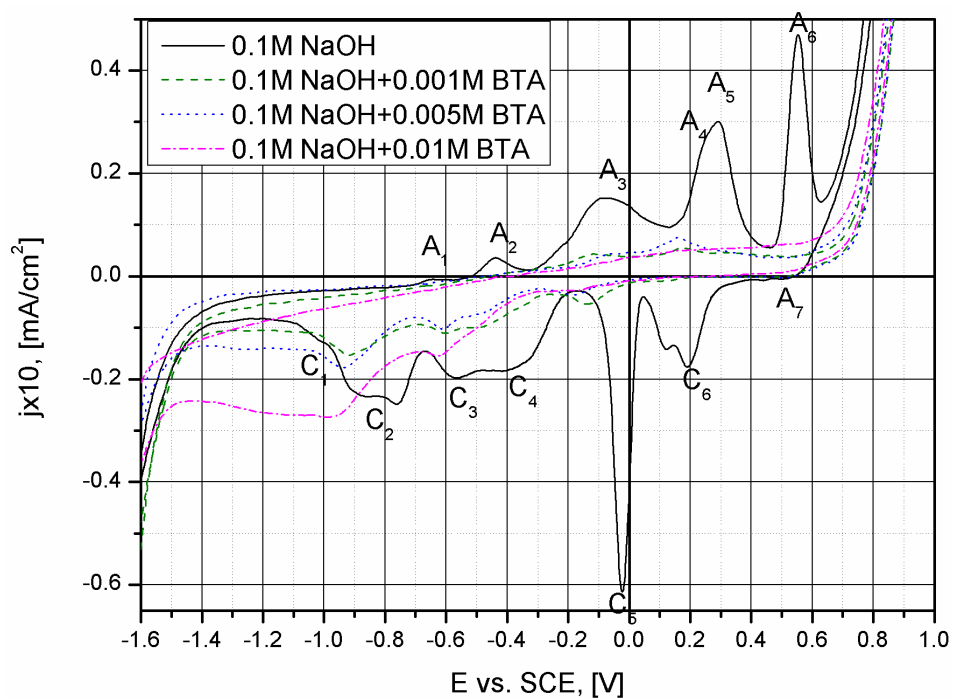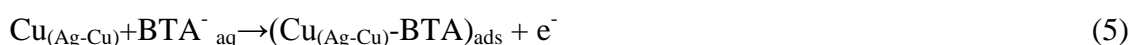

Figure 2. Cyclic voltammetry of AgCu50 in the higher concentration range of BTA, 1.0×10^{-3} - 1.0×10^{-2} mol dm^{-3}. The solid line voltammogram represents the control conditions, the absence of BTA. All voltammograms are produced in 0.1M NaOH at 20 mV s^{-1} scan rate.

For BTA concentrations at 5.0×10^{-4} mol dm^{-3} and below, all current peaks appear at nearly the same potentials as those obtained in the absence of BTA. In the higher concentration range of BTA, Figure 2, all anodic current peaks flattened out to significantly lower levels. The cathodic currents, although also reduced, are distinct and somewhat shifted in negative direction.

Taking into account that no new current peak appears in presence of BTA, it can be assumed that there are no new electrochemical reactions either. In other words, the BTA influences the oxidation processes by blocking the active sites on electrode surface.

The pH of 0.1 mol dm^{-3} NaOH is about 12, and after Tromans [15] diagram, BTA$^-$ species is to be considered as a stable form in the investigated system. Therefore, it can be presumed that with the addition of BTA a CuBTA film is formed on copper and on Ag-Cu alloy by the following reactions:
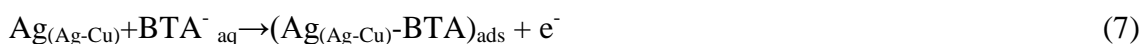
$$Cu_{(Ag-Cu)} + BTA^-_{\,aq} \rightarrow (Cu_{(Ag-Cu)}\text{-}BTA)_{ads} + e^- \qquad (5)$$

or

$$(Cu_{(Ag-Cu)}\text{-}H_2O)_{ads} + BTA^- \rightarrow (Cu_{(Ag-Cu)}\text{-}BTA)_{ads} + H_2O_{aq} + e^- \qquad (6)$$

Copper and silver oxides form at the same time on unoccupied sites.

On silver rich sites of the alloy, it could be expected that AgBTA is formed by similar reactions:

$$Ag_{(Ag-Cu)} + BTA^-_{\,aq} \rightarrow (Ag_{(Ag-Cu)}\text{-}BTA)_{ads} + e^- \qquad (7)$$

or

$$(Ag_{(Ag-Cu)}\text{-}H_2O)_{ads} + BTA^- \rightarrow (Ag_{(Ag-Cu)}\text{-}BTA)_{ads} + H_2O_{aq} + e^- \qquad (8)$$

Simultaneously with reactions (5), (6), (7) and (8), silver oxides Ag$_2$O i AgO are formed, but the mechanism of formation of Ag$_2$O has changed in comparison with the one taking place in the absence of BTA. The oxides of copper and silver form on unoccupied sites until the whole surface is covered with CuBTA and AgBTA complexes.

Surface coverage, θ, is calculated from the equation:

$$\theta = 1 - j_{inh}/j \qquad (9)$$

where j and j_{inh} are current densities in the absence and in the presence of the inhibitor, respectively.

Surface coverage values for the voltage at -0.2 V are given in Table 1.

Table 1. Electrode surface coverage as a function of concentration of BTA

cBTA [M]	0.00005	0.0001	0.0005	0.001	0.005	0.01
θ	0	0.1176	0.16176	0.6176	0.735	0.7647

The surface coverage increases with the increase of BTA concentration, leading to the oxidation protection improvement via formation of CuBTA and AgBTA complexes.

The adsorption of BTA is modelled by using Langmuir isotherm equation [42,43]:

$$\theta/(1-\theta) = Kc \tag{10}$$

where: - θ is the surface coverage calculated from equation (9)

K is the equilibrium adsorption constant,

c is concentration of the inhibitor.

Langmuir isotherm can be presented also in the following form:

$$c/\theta = 1/K + c \tag{11}$$

The equilibrium adsorption constant depends on Gibbs free energy of adsorption [41,42]:

$$K = (1/55.5)\exp(-\Delta G^{o}_{ads}/RT) \tag{12}$$

where 55.5 is the concentration of water in solution in mol dm^{-3}, R is the universal gas constant in J $mol^{-1}K^{-1}$, T is thermodynamic temperature in K and ΔG^{o}_{ads} - Gibbs energy of adsorption.

The plot c/θ versus the concentration of BTA yields straight line, as presented in Figure 3.
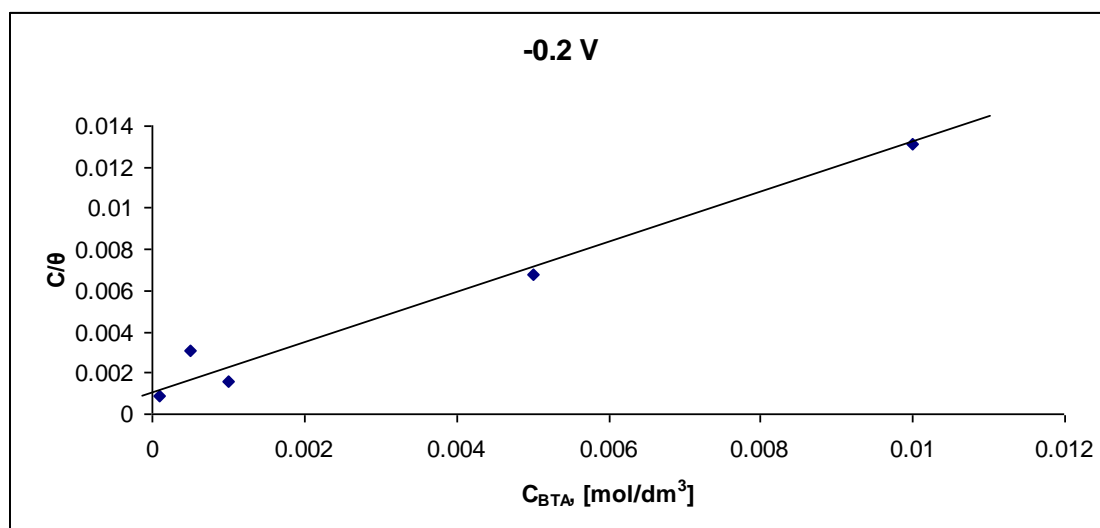
Figure 3. Dependence of c/θ on concentration of benzotriazole.

The linear dependence between c/θ and concentration of benzotriazole confirms that the adsorption of BTA on surface of Ag-Cu alloy is governed by Langmuir adsorption mechanisms. The intercept on c/θ axes corresponds to the value of 1/K, which when inserted in the equation (12) gives ΔG^{o}_{ads} = -27 kJ mol^{-1}. This value points out that the adsorption of BTA on investigated alloy is a spontaneous process involving chemisorption mechanisms.

3.2. Potentiostatic measurements

Potentiostatic measurements were conducted at potentials corresponding to the anodic current peaks A_3, A_5 and A_6 during 100 seconds.

Potentiostatic curves obtained for AgCu50 alloy in 0.1 mol dm^{-3} NaOH with different concentrations of BTA are presented in Figure 4. The potential fixed at -100 mV (SCE) corresponds to the peak A_3. The current obtained in pure sodium hydroxide solution increases in the initial stage, i.e. during the surface formation of copper oxides. These oxides protect alloy from further oxidation and current density remains constant after reaching some maximum value. That steady state value is very low (in the order of magnitude of 100 mA cm^{-2}) With the addition of BTA the current densities become lower because Cu(I)BTA film forms and protects the alloy from oxidation [7]. At low concentrations of benzotriazole, from 5x10^{-5} mol dm^{-3} to 1x10^{-4} mol dm^{-3}, the anodic current flow is very similar to the one obtained in pure sodium hydroxide. This current slowly increases in the first 60 s, reaches a maximum and this maximum becomes a steady state current value. At BTA concentrations higher than 10^{-4} mol dm^{-3}, no anodic current appears during the entire time of reaction. Therefore, in the higher concentration range of BTA, the alloy is fully protected from corrosion.
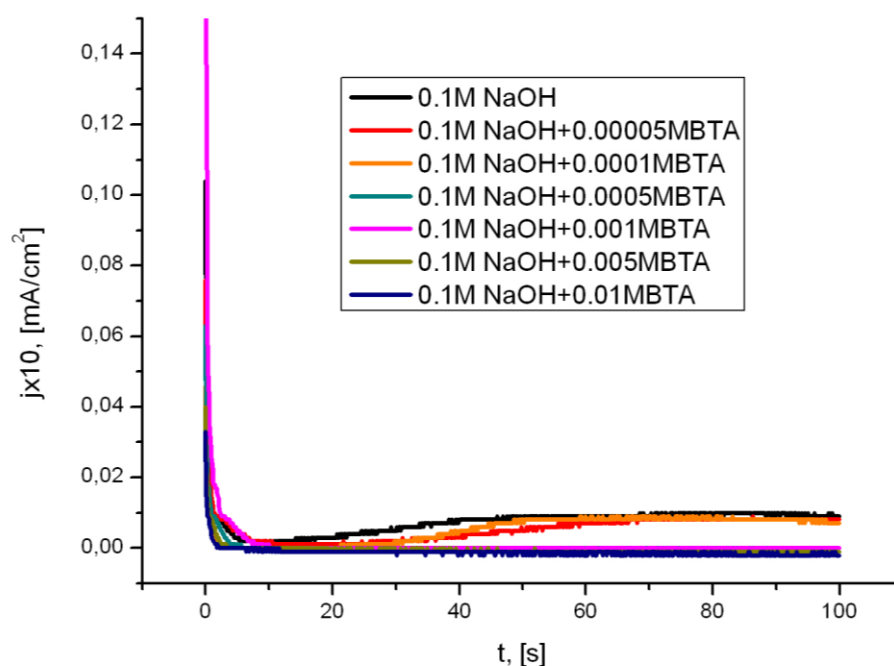

Figure 4. Potentiostatic curves of AgCu50 as a function of benzotriazole concentration in 0.1 mol dm^{-3} NaOH. Potential held constant at -100 mV vs. SCE.

Figure 5 shows the SEM photomicrograph, with EDS spectrum, of AgCu50 alloy after potentiostatic oxidation at -100 mV (SCE) for 100 seconds in solution of 0.1 mol dm^{-3} NaOH + 0.001 mol dm^{-3} BTA. Two different phases are clearly visible. During cooling of liquid Ag-Cu alloy, α-Cu is the first phase to solidify (primary α-Cu) , leaving most of Ag in the liquid phase. Just below the eutectic temperature, the remaining liquid phase, which is now of eutectic composition, redistrubutes itself into eutectic microstructure made of alterating eutectic α-Cu and β-Ag lamellae. (There is a compositional difference between primary-α and eutectic-α phases). In Fig. 5, the dark lamellae represent copper rich α-phase.
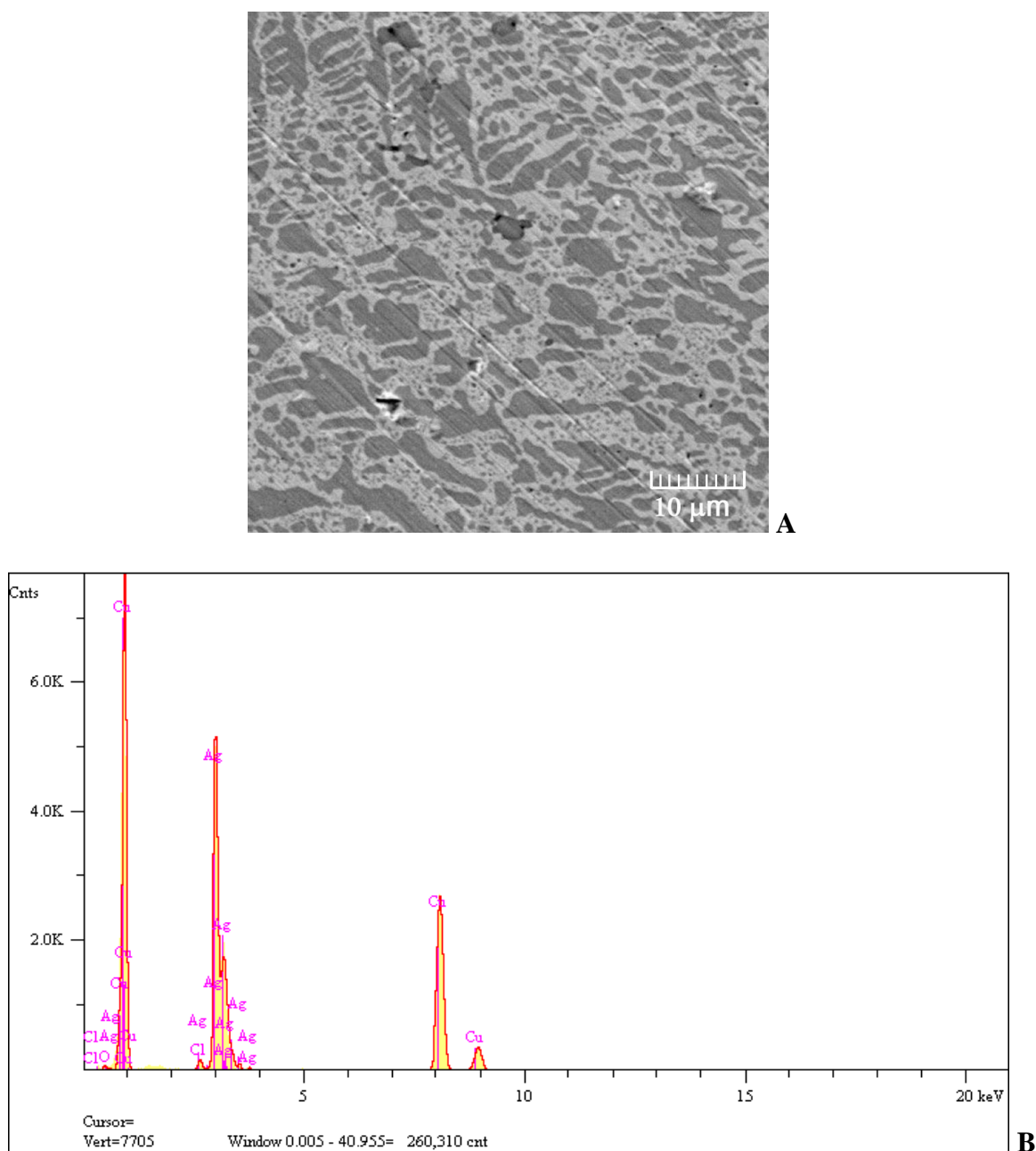
Figure 5. SEM photomicrograph (a) with EDS spectrum (b) of AgCu50 alloy after potentiostatic oxidation at -100 mV (SCE) for 100 seconds in 0.1 mol dm^{-3} NaOH + 0.001 mol dm^{-3} BTA.

Energy dispersive X-ray spectroscopy pointed out that concentration of oxygen on electrode surface was about 0.15 % (Table 2). This value is small enough to be ingnored, so it may be concluded that BTAH in concentration of 0.001 M fully protects AgCu50 alloy from corrosion in 0.1 mol dm^{-3} NaOH. Data derived from the EDS spectrum presented in Figure 5b are sumarized in Table 2.

Table 2. Results derived from EDS spectrum given in Fig. 5b.

Elt.	Decon	Atomic Ratio	Conc	Units	Bkg Error 2-sig
O	Gauss	1.0000	0.152	wt. %	0.206
Cl	Gauss	0.0000	0.000	wt. %	0.298
Cu	Gauss	63.8866	38.477	wt. %	0.197
Ag	Gauss	60.0311	61.372	wt. %	0.365
			100.000	wt. %	

Figure 6 shows potentiostatic curves obtained for AgCu50 alloy at 300 mV vs. SCE, which corresponds to potential of peak A$_5$, for 100 seconds in solution of 0.1 mol dm^{-3} NaOH with different concentrations of BTA. The current peak A$_5$ is related to oxidation of silver to silver(I) oxide. However, it must be taken into account that in the potentiostatic measurements, becuase the alloy is immediately imposed to the set potential, there was no time for prior formation of copper oxides. It means that at this potential the conditions exist for copper to be oxidized sumultaneously with silver.
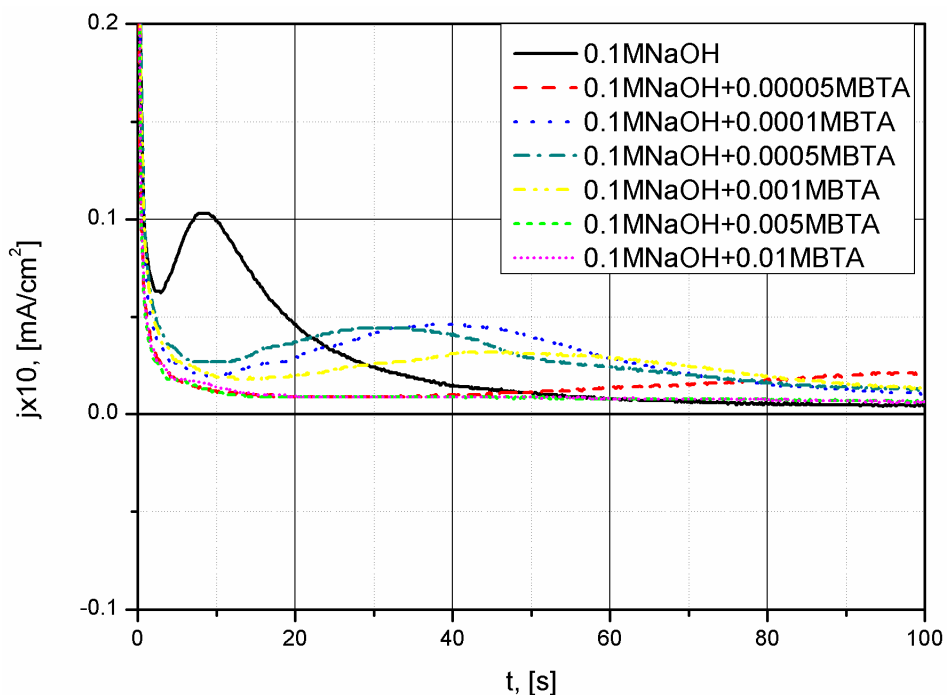

Figure 6. Potentiostatic curves of AgCu50 as a function of benzotriazole concentration in 0.1 mol dm^{-3} NaOH. Potential held constant at 300 mV vs. SCE.

The shape of potentiostatic curves in Figure 6, consisting of electrode discharge and overlap of diffusional zones, strongly indicate the typical nucleation and 3D growth mechanisms [36]. In the absence of BTA, the nucleation stage (first few seconds) and the diffusional zone overlap stage (at about 10 seconds) are sharply defined for the process of oxidation in 0.1M NaOH (BTA is absent). In the presence of benoztriazole, the characteristic stages for nucleationa and 3D growth are broad, nevertheless distinguishable, except for very high concentration of BTA, 5×10^{-3} mol dm^{-3} and 1×10^{-2} mol dm^{-3}. The low and constant transient current for the high concentrations of BTA demostrate the efficacy of corrosion protection by Cu(I)BTA and AgBTA films.

Using the data obtained from Figure 6, Figure 7 represents the current density reached after 100s in dependence on BTA concentration in log j = f (log C_{BTA}) coordinate system. A third degree polynomial approximately fits the data.
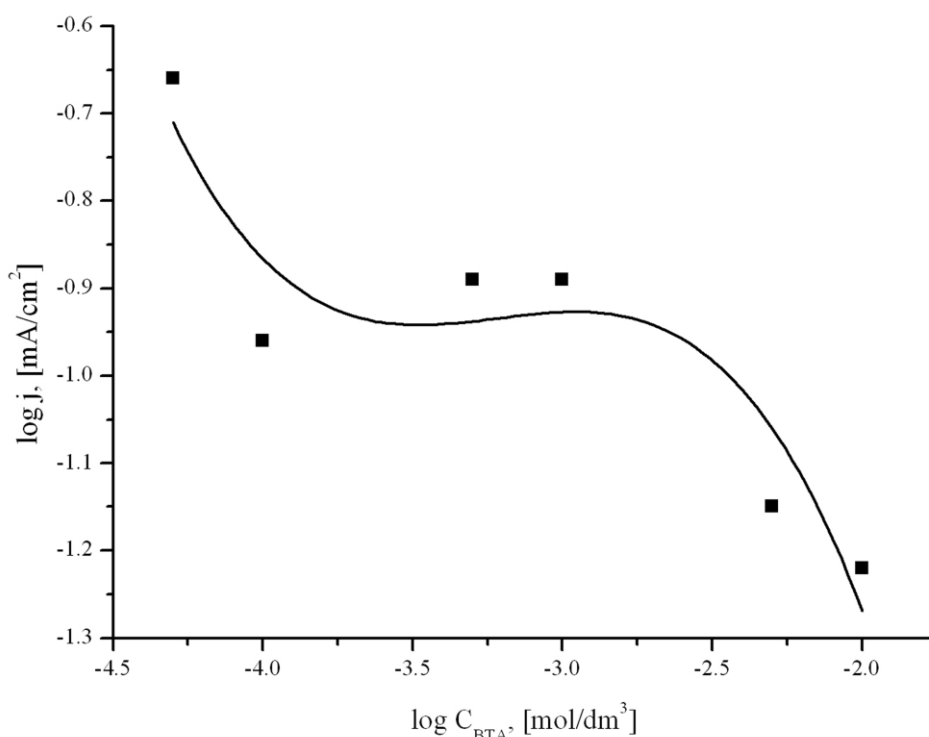

Figure 7. Reaction order plot: log(stationary current density reached after 100s at 300 mV) vs. log(BTA concentration).

The dependence log j = f (log C_{BTA}) shows that the protection mechanisms are dependent on the initial concentration of BTA. Current density sharply decreases with the increase of BTA concentration from 5×10^{-5} mol dm^{-3} to 1×10^{-4} mol dm^{-3}. In the concentration range of BTA between 1×10^{-4} mol dm^{-3} and 1×10^{-3} mol dm^{-3}, the current density remains almost constant, while for concentrations higher than 1×10^{-3} mol dm^{-3}, the decrease in the log j = f(log C_{BTA}) coordinate system is linear.
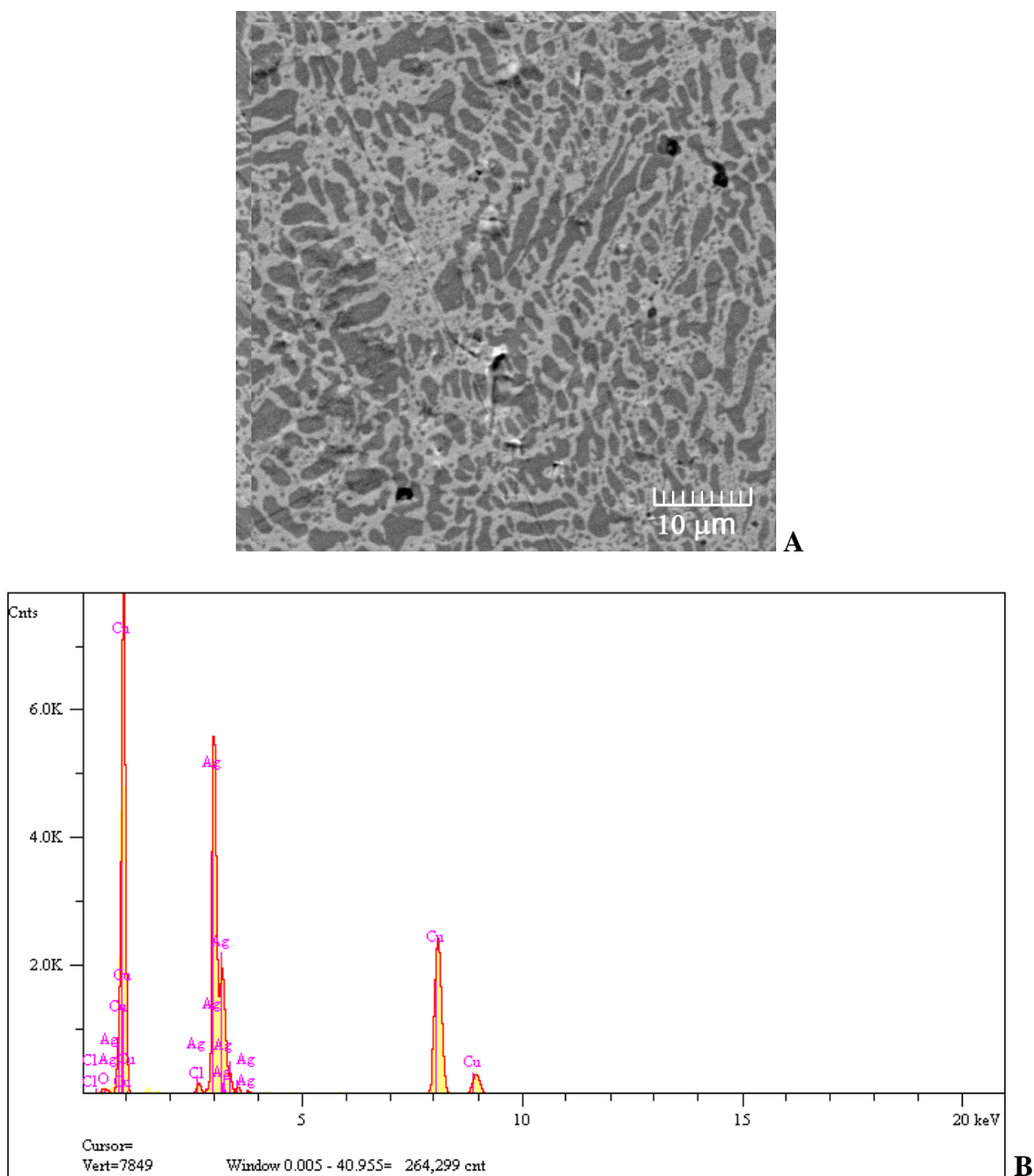
Figure 8. SEM image (a) with EDS spectrum (b) of AgCu50 alloy after potentiostatic oxidation at 300 mV vs. SCE for 100 s in 0.1 mol dm^{-3} NaOH + 0.001 mol dm^{-3} BTA.

Table 3. Results derived from EDS spectrum given in Fig. 8b.

Elt.	Decon	Atomic Ratio	Conc	Units	Bkg Error 2-sig
O	Gauss	1.0000	0.159	wt. %	0.314
Cl	Gauss	0.0000	0.000	wt. %	0.464
Cu	Gauss	56.1395	35.472	wt. %	0.298
Ag	Gauss	60.0140	64.369	wt. %	0.570
			100.000	wt. %	

Figure 8 shows the SEM photomicrograph with the EDS spectrum of surface of $Cu_{50}Ag_{50}$ alloy after potentiostatic oxidation at 300 mV (SCE) for 100 seconds in the solution of 0.1 mol dm^{-3} NaOH + 0.001 mol dm^{-3} BTA. According to the energy dispersive X-ray spectroscopy, the concentration of oxygen on electrode surface (Table 3) is about the same as after oxidation at -100 mV (Table 2). The low oxygen concentration value confirms that CuBTA and AgBTA films do not allow copper and silver oxides to be formed.

Potentiostatic curves recorded for AgCu50 alloy in 0.1 mol dm^{-3} NaOH with different concentrations of BTA at 580 mV (SCE), which corresponds to the current peak A_6, are presented in Figure 9. For these conditions, the current density decreases monotonously until it reaches stationary state [34, 40]. By using the data in Fig. 9, the current densities reached after 100 seconds for each BTA concentration studied. Fig. 10 is constructed in the log j = f (log C_{BTAH}) coordinate system. As previously, the data can be approximately fitted by a third degree polynomial. There are three clearly distinctive regions, as in Figure 7. In the first region, up to $1x10^{-4}$ mol dm^{-3} BTA, the presence of benzotriazole leads to a sharp decrease of current density. In the second region, where the concentration is from $1x10^{-4}$ mol dm^{-3} to $5x10^{-3}$ mol dm^{-3}, the presence of benzotriazole has no significant influence on the current density. Finally, for higher than $5x10^{-3}$ mol dm^{-3} BTAH concentrations, the linear relationship in the log j = f (log C_{BTA}) plot indicates a more intensive formation of protective complexes.
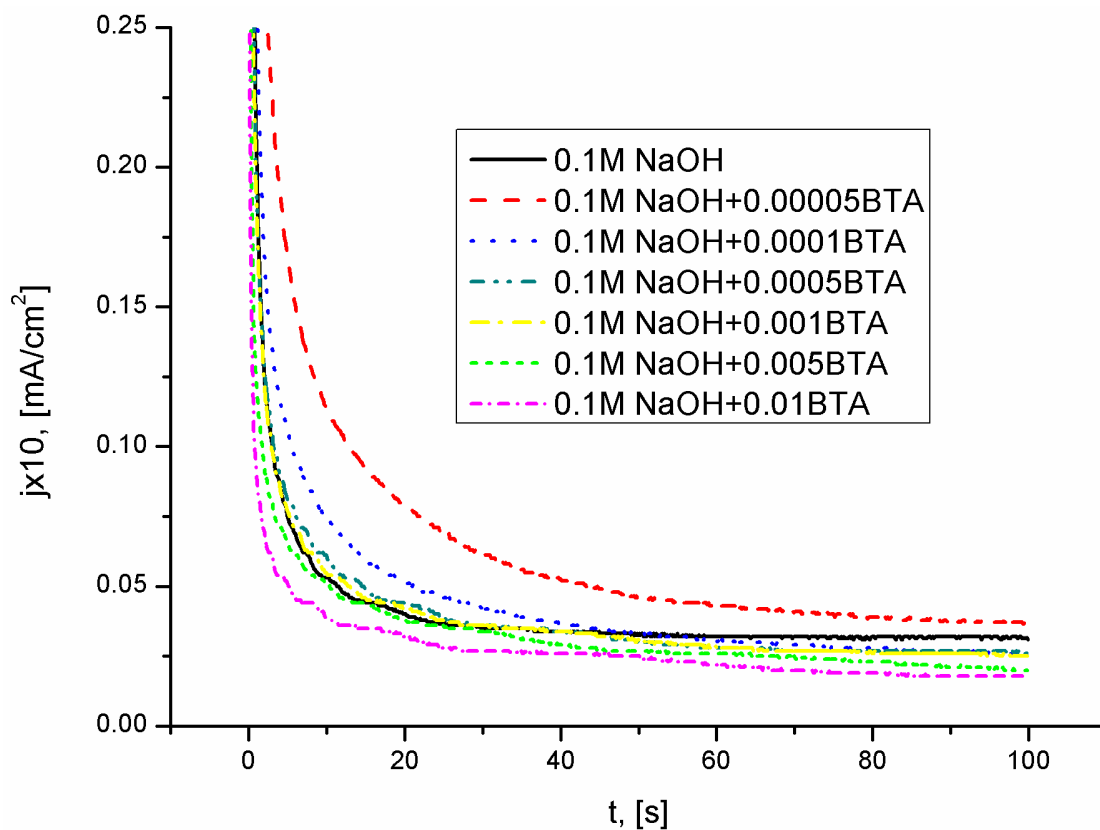

Figure 9. Potentiostatic curves of AgCu50 a function of benzotriazole concentration in 0.1 mol dm^{-3} NaOH. Potential held constant at 580 mV vs. SCE
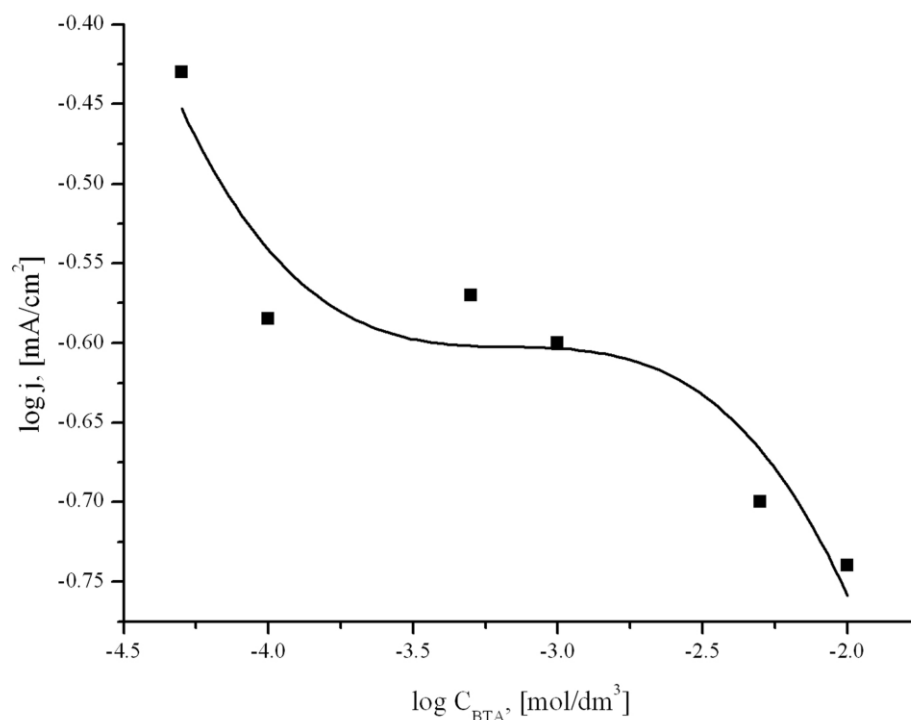
Figure 10. Reaction order plot: log(stationary current density reached after 100s at 580 mV) vs. log(BTA concentration).

4. CONCLUSIONS

The electrochemical investigation of AgCu50 alloy in 0.1 mol dm^{-3} NaOH showed that six anodic and six corresponding cathodic current peaks appear at the same potentials regardless if the inhibitor BTA is present, or absent. Although the presence of BTA has no effect on development of new reactions, its presence, however, is effective with regard to the intensity of anodic current peaks, which decrease with the increase of BTA concentration, demonstrating corrosion inhibition properties. The inhibition is achieved via filming of Ag-Cu alloy surface by the species of CuBTA and AgBTA. The surface coverage increases with the increase of benzotriazole concentration, leading to the increased corrosion protection. The found value for Gibbs free energy of adsorption, -27 kJ mol^{-1}, indicates that the interaction between Ag-Cu alloy and benzotriazole is governed by chemisorption.

According to potentiostatic measurements, and functional relationship logj = f(logCBTA), it can be concluded that the inhibitory effects of BTA are dependent upon its concentration in the electrolyte. In the low concentration range of BTA, 5.0×10^{-5} mol dm^{-3} – 1.0×10^{-4} mol dm^{-3} BTA, there is a rapid decrease of current density. No further decrease of current density is achieved until 5×10^{-5} mol dm^{-3}, after which the log of current density decreases linearly with the logarithm of BTA concentration.

SEM photomicrographs and EDS analysis have confirmed that the formation of copper and silver oxides in the presence of BTA is negligible.

References

1. M. M. Antonijevic, M. B. Petrovic, *Int. J. Electrochem. Sci*.3, 1 (2008) 1
2. R. Subramanian, V. Lakshminarayanan, *Corros. Sci*. 44, 3 (2002) 535
3. J. Bartley, N. Huynh, S.E. Bottle, H. Flitt, T. Notoya, D.P. Schweinsberg, *Corros. Sci*. 45 (2003) 81
4. B.H. Loo, A. Ibrahim, M.T. Emerson, *Chem. Phys. Letters* 287 (1998) 449
5. P. Yu, D-M Liao, Y-B Luo, Z-G Chen, Corrosion 59, 4 (2003) 314
6. A.Arancibia, J. Henriquez-Roman, M. A. Páez, L. Padilla-Campos, J. H. Zagal, J. Costamagna, G. Cárdenas-Jirón, *J. Solid State Electrochem*. 10 (2006) 894
7. Abdullah A. M.,. Al-Kharafi F. M,. Ateya B. G, *Scripta Mater*. 54 (2006) 1673
8. Modestov A. D., Zhou G.-D, Wu Y.-P., Notoya T., Schweinsberg D. P., *Corros. Sci*. 36, 11 (1994) 1931
9. G-D Zhou, H. Shao, B. H. Loo, *J. Eleetroanal.Chem*. 421 (1997) 129
10. S. Mamas, T. Kıyak, M. Kabasakaloglu, A. Koc, *Mater. Chem. Phys*. 93 (2005) 41
11. D-Q. Zhang, L-X. Gao, G-D. Zhou, *J. Appl. Electrochem*. 33, (2003) 361
12. R.F.V. Villamil., G.G.O. Cordeiro, J. Matos, E. D'Elia, Agostinho S.M.L., *Mater. Chem. Phys*. 78 (2002) 448
13. J.B. Matos, E. D'Elia, O.E. Barcia, O.R. Mattos, N. Pebere, B. Tribollet, *Electrochim. Acta* 46 (2001) 1377
14. D. Tromans, R. Sun, *J. Electrochem. Soc*. 138,11 (1991) 3235
15. D. Tromans , *J. Electrochem. Soc*. 145, 3 (1998) 42
16. D. M. Bastidas, *Surf. Interface Anal*. 38, (2006) 1146
17. E. Cano, *Adsorption* 10 (2004) 219
18. G.A. Hope, K. Watling, R. Woods, *J. Appl. Electrochem*. 31 (2001) 703
19. M. Rajeswarana, T. N. Blantona, D. J. Giesena, D. R. Whitcomba, N. Zumbulyadisa, B. J. Antaleka, M. M. Neumannc, S. T. Misture, *J. Solid State Chem*. 179 (2006) 1053
20. Z. Stević, M. Rajčić-Vujasinović, *Chemical Industry*, 61 (2007) 1
21. J. Kunze, V. Maurice, L. H. Klein, H. H. Strehblow, P. Marcus, *Electrochim. Acta* 48 (2003) 1157
22. H. H. Strehblow, V. Maurice, P. Marcus, Electrochim. Acta 46 (2001) 3755
23. S. Nakayama, T. Kaji, T. Notoya, T. Osakai, *Electrochim. Acta* 53 (2008) 3493
24. D. Hecht, H.-H. Strehblow, *J. Electroanal. Chem*. 436 (1997) 109
25. S. S. Abd El Rehim, H.H. Hassan, M. A. M. Ibrahim, M. A. Amin, *Monatshefte Chemie* 129 (1998) 1103
26. J. Kunze, H.H. Strehblow, G. Staikov, *Electrochem. Commun*. 6 (2004) 132
27. N. Iwasaki, Y. Sasaki, Y. Nishina, *Surf. Sci*. 158 (1985) 352
28. M. Rajčić-Vujasinović, S. Nestorović, V. Grekulović, I. Marković, Z. Stević, *Metall. Mat. Trans*. B, 41 (2010) 955
29. H. H. Strehblow, B. Titze, *Electrochim. Acta* 25 (1980) 839
30. J. Kunze, V. Maurice, L. H. Klein, H. H. Strehblow, P. Marcus, *J. Electroanal. Chem*. 554-555 (2003) 113
31. S. M. Milić, M. M. Antonijević, *Corros. Sci*., 51 (2009) 28
32. S. M. Abd El Haleem, E. E. Abd El Aal, *Corrosion 6*2 (2006) 121
33. M. Rajcić-Vujasinović, S. Nestorović, V. Grekulović, I. Marković, Z. Stević, *Corrosion*, 66 (2010) 105004-1

34. A.M. Zaky, F. H. Assaf , S. S. Abd El Rehim, B. M. Mohamd, *Appl. Surf. Sci*. 221 (2004) 349
35. B. M. Jović, V.D. Jović, *J. Serb. Chem. Soc*. 69 (2004) 153
36. T. Uk Hur, W . Sub Chung, *J. Electrochem. Soc*. 152 (2005) A179
37. J. Ambrose, R. G. Barradas, *Electrochim. Acta* 19 (1974) 781
38. G. T. Burstein, R. C. Newman, *Electrochim. Acta* 25 (1980) 1009
39. D. Hecht, P. Borthen, H.H. Strehblow, *Surf. Sci.* 365 (1996) 263
40. O. A. Hazzazi, A. M. Zaky, M. A. Amin, S. S. Abd El Rehim, *Int. J. Electrochem. Sci*.3 (2008) 489
41. P. Stonehart, *Electrochim. Acta* 13 (1968) 1789
42. M. Ehteshamzade, T. Shahrabi, M. G. Hosseini, *Appl. Surf. Sci*. 252 (2006) 2949
43. T. Kosec, I. Milosev, B. Pihlar, *Appl. Surf. Sci*. 253 (2007) 8863